Eur. Phys. J. B **18**, 703–712 (2000)

THE EUROPEAN PHYSICAL JOURNAL B

EDP Sciences

Field-dependent quantum nucleation of antiferromagnetic bubbles

Rong Lü[a], Yi Zhou, Jia-Lin Zhu, and Bing-Lin Gu

Center for Advanced Study, Tsinghua University, Beijing 100084, PR China

Received 13 June 2000 and Received in final form 24 October 2000

Abstract. The phenomenon of quantum nucleation is studied in a nanometer-scale antiferromagnet with biaxial symmetry in the presence of a magnetic field at an arbitrary angle. Within the instanton approach, we calculate the dependence of the rate of quantum nucleation and the crossover temperature on the orientation and strength of the field for bulk solids and two-dimensional films of antiferromagnets, respectively. Our results show that the rate of quantum nucleation and the crossover temperature from thermal-to-quantum transitions depend on the orientation and strength of the field distinctly, which can be tested with the use of existing experimental techniques.

PACS. 75.45.+j Macroscopic quantum phenomena in magnetic systems – 73.40.Gk Tunneling – 75.30.Gw Magnetic anisotropy – 75.50.Ee Antiferromagnetics

One of the most striking manifestations of the quantum character of nature is quantum tunneling of particles. Following the idea suggested by Caldeira and Leggett [1], the tunneling of macroscopic object, known as Macroscopic Quantum Tunneling (MQT), has become one of the most fascinating phenomena in condensed matter physics. During the last decade, the problem of quantum tunneling of magnetization in nanometer-scale magnets has attracted a great deal of theoretical and experimental interest [2]. The magnetic MQT includes quantum reversal of the magnetization (or the Néel) vector in small single-domain ferromagnets (or antiferromagnets), quantum nucleation of magnetic bubbles, quantum depinning of domain walls from defects in bulk magnets, and resonant spin tunneling in molecular magnetic clusters [2]. MQT in magnetic systems are interesting from a fundamental point of view as it can extend our understanding of the limits between quantum and classical physics. On the other hand, MQT is important to the reliability of small magnetic units in memory devices and the designing of quantum computers in the future. And the measurement of magnetic MQT quantities such as the tunneling rates could provide independent information about microscopic parameters such as the magnetocrystalline anisotropies and the exchange constants. All this makes magnetic quantum tunneling an exciting area for theoretical research and a challenging experimental problem.

The problem of quantum nucleation of a stable phase from a metastable one in ferromagnetic films is an interesting fundamental problem which allows direct comparison between theory and experiment [3]. Consider a ferromagnetic film with its plane perpendicular to the easy axis determined by the magnetocrystalline anisotropy energy depending on the crystal symmetry. A magnetic field $\mathbf{H}$ is applied in a direction opposite to the initial easy direction of the magnetization $\mathbf{M}$, which favors the reversal of the magnetization. The reversal occurs *via* the nucleation of a critical bubble, which then the nucleus does not collapse, but grows unrestrictedly in volume. If the temperature is sufficiently high, the nucleation of a bubble is a thermal overbarrier process, and the rate of thermal nucleation follows the Arrhenius law $\Gamma_T \exp(-U/k_{\rm B}T)$, with $k_{\rm B}$ being the Boltzmann constant and U being the height of energy barrier. In the limit of $T \to 0$, the nucleation is purely quantum-mechanical and the rate goes as $\Gamma_Q \exp(-\mathcal{S}_{\rm cl}/\hbar)$, with $\mathcal{S}_{\rm cl}$ being the classical action or the WKB exponent which is independent of temperature. Because of the exponential dependence of the thermal rate on T, the temperature $T_{\rm c}$ characterizing the crossover from quantum to thermal regime can be estimated as $k_{\rm B}T_{\rm c} = \hbar U/\mathcal{S}_{\rm cl}$.

A few theoretical studies of the problem of quantum nucleation have been around for some time. Privorotskii estimated the exponent in the rate of quantum nucleation based on the dimensional analysis [4]. Chudnovsky and Gunther studied the quantum nucleation of a thin ferromagnetic film in a magnetic field along the opposite direction to the easy axis at zero temperature by applying the instanton method [5]. Later, Ferrera and Chudnovsky extended the quantum nucleation to a finite temperature [6]. Kim studied the effect of an arbitrarily directed magnetic field on the quantum nucleation of magnetization [7]. The phenomenon of quantum nucleation was also found in nanometer-scale antiferromagnets [8–10], where

[a] e-mail: rlu@castu.tsinghua.edu.cn

the Néel vector is the tunneling entity. Theoretical studies on small single-domain antiferromagnets showed that quantum tunneling should show up at higher temperatures and higher frequencies than in single-domain ferromagnets of similar size [2]. This makes nanometer-scale antiferromagnets more interesting for experimental test.

Up to now theoretical studies on quantum nucleation in antiferromagnets [8–10] were confined to the condition that the metastable state is caused by the magnetocrystalline anisotropy, which is not easily controlled in experiments. It is well-known that a magnetic field is a good external parameter to make the phenomenon of MQT observable. The purpose of this paper is to extend the previous considerations [8–10] to a system with a magnetic field applied in an arbitrary direction between perpendicular and opposite to the initial easy axis ($\widehat{\mathbf{z}}$-axis). By applying the instanton method in the spin-coherent-state path-integral representation, we present the numerical results for the WKB exponent in quantum nucleation of a thin ferromagnetic film with the magnetic field applied in a range of angles $\pi/2 < \theta_H < \pi$ and $\theta_H = \pi$ respectively, where θ_H is the angle between the initial easy axis ($\widehat{\mathbf{z}}$-axis) and the field. We also discuss the θ_H dependence of the crossover temperature T_c from purely quantum nucleation to thermally assisted processes. Our results show that the distinct angular dependence, together with the dependence of the WKB exponent on the strength of the external magnetic field, may provide an independent experimental test for quantum nucleation in an antiferromagnetic film.

For a spin tunneling problem, the rate of magnetization reversal by quantum tunneling can be determined by the imaginary-time transition amplitude from an initial state $|i\rangle$ to a final state $|f\rangle$ as

$$U_{fi} = \langle f| \, \mathrm{e}^{-\mathcal{H}T} \, |i\rangle = \int \mathcal{D}\left\{\mathbf{M}\left(\mathbf{r},\tau\right)\right\} \exp\left(-\mathcal{S}_{\mathrm{E}}/\hbar\right), \quad (1)$$

where $\mathcal{S}_{\mathrm{E}}$ is the Euclidean action which includes the Euclidean Lagrangian density $\mathcal{L}_{\mathrm{E}}$ as

$$\mathcal{S}_{\mathrm{E}} = \int \mathrm{d}\tau \mathrm{d}^3\mathbf{r}\mathcal{L}_{\mathrm{E}}. \quad (2)$$

The system of interest is an antiferromagnet of about 5–10 nm in radius at a temperature well below its anisotropy gap. According to the two-sublattice model [8], there is a strong exchange energy $\mathbf{m}_1 \cdot \mathbf{m}_2/\chi_\perp$ between two sublattices, where $\mathbf{m}_1$ and $\mathbf{m}_2$ are the magnetization vectors of the two sublattices with large, fixed and unequal magnitudes, and $\chi_\perp$ is the transverse susceptibility. In the semiclassical regime and using the spin-coherent-state path-integral, one gets the Euclidean Lagrangian density for antiferromagnets (neglecting dissipation with the environment) as [8–10]

$$\begin{aligned}\mathcal{L}_{\mathrm{E}}[\theta(\mathbf{r},\tau),\phi(\mathbf{r},\tau)] &= \mathrm{i}\frac{m_1+m_2}{\gamma}\left(\frac{\mathrm{d}\phi}{\mathrm{d}\tau}\right) - \mathrm{i}\frac{m}{\gamma}\left(\frac{\mathrm{d}\phi}{\mathrm{d}\tau}\right)\cos\theta \\ &+ \frac{\chi_\perp}{2\gamma^2}\left[\left(\frac{\mathrm{d}\theta}{\mathrm{d}\tau}\right)^2 + \left(\frac{\mathrm{d}\phi}{\mathrm{d}\tau}\right)^2\sin^2\theta\right] \\ &+ \frac{1}{2}\alpha\left[(\nabla\theta)^2 + (\nabla\phi)^2\sin^2\theta\right] + E(\theta,\phi), \quad (3)\end{aligned}$$

where γ is the gyromagnetic ratio, α is the exchange constant [11], and $\tau = \mathrm{i}t$ is the imaginary-time variable. The $E(\theta,\phi)$ term includes the magnetocrystalline anisotropy and the Zeeman energies. $m = m_1 - m_2 = \hbar\gamma s$, where s is the excess spin due to the noncompensation of two sublattices. The polar coordinate θ and the azimuthal coordinate ϕ in the spherical coordinate system with $\mathbf{l}\cdot\widehat{\mathbf{z}} = \cos\theta$, $\mathbf{l}$ is the Néel vector of unit length and $\widehat{\mathbf{z}}$ is a unit vector along the $\mathbf{z}$-axis. The first term in equation (3) is a total imaginary-time derivative, which has no effect on the classical equations of motion, but it is crucial for the spin-parity effects [2,8,12–18]. However, for the closed instanton trajectory described in this paper (as shown in the following), this time derivative gives a zero contribution to the path integral, and therefore can be omitted. In the semiclassical limit, the rate of quantum nucleation, with an exponential accuracy, is given by

$$\Gamma_Q \exp\left[-\mathcal{S}_{\mathrm{E}}^{\min}/\hbar\right], \quad (4)$$

where $\mathcal{S}_{\mathrm{E}}^{\min}$ is obtained along the trajectory that minimizes the Euclidean action $\mathcal{S}_{\mathrm{E}}$.

In this paper, we study the quantum nucleation of the Néel vector in antiferromagnets with biaxial symmetry in the presence of a magnetic field at arbitrary angles in the ZX plane, which has the following magnetocrystalline anisotropy energy

$$\begin{aligned}E(\theta,\phi) &= K_1\sin^2\theta + K_2\sin^2\theta\sin^2\phi \\ &- mH_x\sin\theta\cos\phi - mH_z\cos\theta, \quad (5)\end{aligned}$$

where K_1 and K_2 are the longitudinal and the transverse anisotropy coefficients respectively, and $K_1 > 0$. In the absence of the magnetic field, the easy axes of this system are $\pm\widehat{\mathbf{z}}$ for $K_1 > 0$. And the field is applied in the ZX plane at $\pi/2 < \theta_H < \pi$. By introducing the dimensionless parameters as

$$\overline{K}_2 = K_2/2K_1, \quad \overline{H}_x = H_x/H_0, \quad \overline{H}_z = H_z/H_0. \quad (6)$$

Equation (5) can be rewritten as

$$\begin{aligned}\overline{E}(\theta,\phi) &= \frac{1}{2}\sin^2\theta + \overline{K}_2\sin^2\theta\sin^2\phi \\ &- \overline{H}_x\sin\theta\cos\phi - \overline{H}_z\cos\theta + \overline{E}_0, \quad (7)\end{aligned}$$

where $E(\theta,\phi) = 2K_1\overline{E}(\theta,\phi)$, and $H_0 = 2K_1/m$. At finite magnetic field, the plane given by $\phi = 0$ is the easy plane, on which $\overline{E}(\theta,\phi)$ reduces to

$$\overline{E}(\theta,\phi=0) = \frac{1}{2}\sin^2\theta - \overline{H}\cos(\theta-\theta_H). \quad (8)$$

We denote θ_0 to be the initial angle and θ_c the critical angle at which the energy barrier vanishes when the external magnetic field is close to the critical value $\overline{H}_c(\theta_H)$ (to be calculated in the following). Then, the initial angle θ_0 satisfies $\left[\mathrm{d}\overline{E}(\theta,\phi=0)/\mathrm{d}\theta\right]_{\theta=\theta_0}=0$, the critical angle θ_c and the dimensionless critical field $\overline{H}_c$ satisfy both $\left[\mathrm{d}\overline{E}(\theta,\phi=0)/\mathrm{d}\theta\right]_{\theta=\theta_c,\overline{H}=\overline{H}_c}=0$ and $\left[\mathrm{d}^2\overline{E}(\theta,\phi=0)/\mathrm{d}\theta^2\right]_{\theta=\theta_c,\overline{H}=\overline{H}_c}=0$, which leads to

$$\frac{1}{2}\sin(2\theta_0)+\overline{H}\sin(\theta_0-\theta_H)=0, \tag{9a}$$

$$\frac{1}{2}\sin(2\theta_c)+\overline{H}_c\sin(\theta_c-\theta_H)=0, \tag{9b}$$

$$\cos(2\theta_c)+\overline{H}_c\cos(\theta_c-\theta_H)=0. \tag{9c}$$

After some algebra, the dimensionless critical field $\overline{H}_c(\theta_H)$ and the critical angle θ_c are found to be

$$\overline{H}_c=\left[(\sin\theta_H)^{2/3}+|\cos\theta_H|^{2/3}\right]^{-3/2}, \tag{10a}$$

$$\sin(2\theta_c)=\frac{2|\cot\theta_H|^{1/3}}{1+|\cot\theta_H|^{2/3}}. \tag{10b}$$

Then the critical field of this system is $H_c=\overline{H}_c(2K_1/m)$, where $m=\hbar\gamma s/V$, and s is the excess spin of antiferromagnet due to the noncompensation of two sublattices.

It is noted that for the nanometer-scale antiferromagnet at finite magnetic field, there exists another field $H_{\mathrm{s.f.}}$, known as the spin-flop field, which can rotate the moments of sublattices away from the anisotropy axis. The spin-flop field is defined as $H_{\mathrm{s.f.}}=\sqrt{2H_1H_{\mathrm{ex}}}$, with $H_1=2K_1/m_1$ being the longitudinal anisotropy field, and $H_{\mathrm{ex}}=2J_{\mathrm{ex}}/m_1$ being the exchange field between two sublattices. $m_1=\hbar\gamma S/V$ is the magnetization of one sublattice, where S is the sublattice spin. Typical values of parameters for the antiferromagnetic nanoparticle are $K_1\backsim 10^5$ erg/cm^3 and $\chi_\perp\backsim 10^{-5}$ emu/G cm^3. The particle radius is about 12 nm, the sublattice spin is $S=2\times10^5$, and the excess spin is $s=10^3$. It is easy to obtain that the exchange energy density between sublattices is $J_{\mathrm{ex}}\left(=\hbar^2\gamma^2S^2/V^2\chi_\perp\right)\approx 1.9\times10^{10}$ erg/cm^3, $H_0\,(=2K_1/m)\approx 9.0\times10^4$ G, and $H_{\mathrm{s.f.}}\approx 2.8\times10^5$ G, which shows that the critical field is smaller than the spin-flop field. Therefore, the small $\epsilon=1-\overline{H}/\overline{H}_c$ limit can be performed in calculating the rate of quantum nucleation of the Néel vector, at which the two-sublattice configuration is still valid for antiferromagnets at finite magnetic field.

Now we consider the limiting case that the external applied magnetic field is slightly lower than the critical field, *i.e.*, $\epsilon=1-\overline{H}/\overline{H}_c\ll 1$. At this practically interesting situation, the barrier height is low and the width is narrow, and therefore the tunneling rate is large. Introducing $\eta\equiv\theta_c-\theta_0$ ($|\eta|\ll1$ in the limit of $\epsilon\ll1$), expanding $\left[\mathrm{d}\overline{E}(\theta,\phi=0)/\mathrm{d}\theta\right]_{\theta=\theta_0}=0$ about θ_c, and using the relations $\left[\mathrm{d}\overline{E}(\theta,\phi=0)/\mathrm{d}\theta\right]_{\theta=\theta_c,\overline{H}=\overline{H}_c}=0$ and $\left[\mathrm{d}^2\overline{E}(\theta,\phi=0)/\mathrm{d}\theta^2\right]_{\theta=\theta_c,\overline{H}=\overline{H}_c}=0$, equation (9a) becomes

$$\sin(2\theta_c)\left(\epsilon-\frac{3}{2}\eta^2\right)-\eta\cos(2\theta_c)\left(2\epsilon-\eta^2\right)=0. \tag{11}$$

Simple calculations show that η is of the order of $\sqrt{\epsilon}$. Thus the order of magnitude of the second term in equation (11) is smaller than that of the first term by $\sqrt{\epsilon}$ and the value of η is determined by the first term, which leads to $\eta\simeq\sqrt{2\epsilon/3}$. However, when θ_H is very close to $\pi/2$ or π, $\sin(2\theta_c)$ becomes almost zero, and the first term is much smaller than the second term in equation (11). Then η is determined by the second term when $\theta_H\simeq\pi/2$ or π, which leads to $\eta\simeq\sqrt{2\epsilon}$ for $\theta_H\simeq\pi/2$ and $\eta\simeq0$ for $\theta_H\simeq\pi$. Since the first term in equation (11) is dominant in the range of values, θ_c, which satisfies $\tan(2\theta_c)>O(\sqrt{\epsilon})$, $\eta\simeq\sqrt{2\epsilon/3}$ is valid for $\pi/2+O(\sqrt{\epsilon})<\theta_H<\pi-O(\sqrt{\epsilon})$ by using equation (10b). Therefore, $\eta\simeq\sqrt{2\epsilon}$, 0, and $\sqrt{2\epsilon/3}$ for $\theta_H\simeq\pi/2$, π, and $\pi/2+O(\sqrt{\epsilon})<\theta_H<\pi-O(\sqrt{\epsilon})$, respectively. In this case the potential energy $\overline{E}(\theta,\phi)$ reduces to the following equation in the limit of small ϵ,

$$\overline{E}(\delta,\phi)=\overline{K}_2\sin^2\phi\sin^2(\theta_0+\delta)+\overline{H}_x\sin(\theta_0+\delta)(1-\cos\phi)+\overline{E}_1(\delta), \tag{12}$$

where $\delta\equiv\theta-\theta_0$ ($|\delta|\ll1$ in the limit of $\epsilon\ll1$), and $\overline{E}_1(\delta)$ is a function of only δ given by

$$\overline{E}_1(\delta)=\frac{1}{4}\sin(2\theta_c)\left(3\delta^2\eta-\delta^3\right)+\frac{1}{2}\cos(2\theta_c)\left[\delta^2\left(\epsilon-\frac{3}{2}\eta^2\right)+\delta^3\eta-\frac{1}{4}\delta^4\right]. \tag{13}$$

It can be shown that in the region of $\pi/2+O(\sqrt{\epsilon})<\theta_H<\pi-O(\sqrt{\epsilon})$, $O(\sqrt{\epsilon})<\theta_c<\pi/2-O(\sqrt{\epsilon})$, η and δ are of the order of $\sqrt{\epsilon}$, the second term in equation (13) is smaller than the first term in the small ϵ limit. It is convenient to use the dimensionless variables

$$\mathbf{r}'=\epsilon^{1/4}\mathbf{r}/r_0,\quad \tau'=\epsilon^{1/4}\omega_0\tau,\quad \overline{\delta}=\delta/\sqrt{\epsilon}, \tag{14a}$$

where $r_0=\sqrt{\alpha/2K_1}$, and

$$\omega_0=\frac{2\gamma K_1}{m}\left(\frac{\sin\theta_c}{\overline{H}_x+2\overline{K}_2\sin\theta_c}+\frac{2\chi_\perp K_1}{m^2}\right)^{-1/2}. \tag{14b}$$

Then the Euclidean action (2) for $\pi/2+O\left(\sqrt{\epsilon}\right)<\theta_H<\pi-O\left(\sqrt{\epsilon}\right)$ becomes

$$\begin{aligned}\mathcal{S}_{\mathrm{E}}\left[\overline{\delta}\left(\mathbf{r}',\tau'\right),\phi\left(\mathbf{r}',\tau'\right)\right]=&\frac{r_0^3}{\epsilon\omega_0}\int\mathrm{d}\tau'\mathrm{d}^3\mathbf{r}'\Bigg\{\frac{\chi_\perp}{2\gamma^2}\epsilon^{3/2}\omega_0^2\left(\frac{\partial\overline{\delta}}{\partial\tau'}\right)^2\\&+\frac{\chi_\perp}{2\gamma^2}\epsilon^{1/2}\omega_0^2\sin^2\left(\theta_0+\sqrt{\epsilon\overline{\delta}}\right)\left(\frac{\partial\phi}{\partial\tau'}\right)^2\\&-\mathrm{i}\frac{m}{\gamma}\epsilon\omega_0\sin\left(\theta_0+\sqrt{\epsilon\overline{\delta}}\right)\phi\left(\frac{\partial\overline{\delta}}{\partial\tau'}\right)\\&+2K_1\Bigg[\overline{K}_2'\sin^2\phi\sin^2\left(\theta_0+\sqrt{\epsilon\overline{\delta}}\right)\\&+2\overline{H}_x\sin^2\left(\frac{\phi}{2}\right)\sin\left(\theta_0+\sqrt{\epsilon\overline{\delta}}\right)+\frac{1}{2}\epsilon^{3/2}\left(\nabla'\overline{\delta}\right)^2\\&+\frac{1}{2}\epsilon^{1/2}\sin^2\left(\theta_0+\sqrt{\epsilon\overline{\delta}}\right)\left(\nabla'\phi\right)^2+\frac{A}{4}\epsilon^{3/2}\left(\sqrt{6\overline{\delta}}^2-\overline{\delta}^3\right)\Bigg]\Bigg\},\end{aligned}\tag{15}$$

where $A=\sin\left(2\theta_{\mathrm{c}}\right)$. In equation (15) we have performed the integration by part for the term $-\mathrm{i}\frac{m}{\gamma}\cos\theta\left(\frac{\mathrm{d}\phi}{\mathrm{d}\tau}\right)$ and have neglected the total imaginary-time derivative. In can be showed that for $\pi/2+O\left(\sqrt{\epsilon}\right)<\theta_H<\pi-O\left(\sqrt{\epsilon}\right)$, only small values of ϕ contribute to the path integral, so that one can replace $\sin^2\phi$ in equation (15) by ϕ^2 and neglect the term including $\left(\nabla'\phi\right)^2$ which is of the order ϵ^2 while the other terms are of the order $\epsilon^{3/2}$. Then the Gaussian integration over ϕ leads to

$$\int\mathcal{D}\left\{\delta\left(\mathbf{r}',\tau'\right)\right\}\exp\left(-\frac{1}{\hbar}\mathcal{S}_{\mathrm{E}}^{\mathrm{eff}}\right),\tag{16}$$

where the effective action is

$$\begin{aligned}\mathcal{S}_{\mathrm{E}}^{\mathrm{eff}}\left[\overline{\delta}\left(\mathbf{r}',\tau'\right)\right]=\hbar s\epsilon^{1/2}r_0^3\Bigg(&\frac{\sin\theta_{\mathrm{c}}}{\overline{H}_x+2\overline{K}_2\sin\theta_{\mathrm{c}}}\\&+\frac{2\chi_\perp K_1}{m^2}\Bigg)^{1/2}\int\mathrm{d}\tau'\mathrm{d}^3\mathbf{r}'\Bigg[\frac{1}{2}\left(\frac{\partial\overline{\delta}}{\partial\tau'}\right)^2\\&+\frac{1}{2}\left(\nabla'\overline{\delta}\right)^2+\frac{A}{4}\left(\sqrt{6\overline{\delta}}^2-\overline{\delta}^3\right)\Bigg],\end{aligned}\tag{17}$$

and $s=m/\hbar\gamma$ is the excess spin of antiferromagnets. Introducing the variables $\overline{\tau}=\tau'\sqrt{A}$ and $\overline{\mathbf{r}}=\mathbf{r}'\sqrt{A}$, the effective action (17) is simplified as

$$\begin{aligned}\mathcal{S}_{\mathrm{E}}^{\mathrm{eff}}\left[\overline{\delta}\left(\overline{\mathbf{r}},\overline{\tau}\right)\right]=\hbar s\epsilon^{1/2}r_0^3\frac{1}{A}\Bigg(&\frac{\sin\theta_{\mathrm{c}}}{\overline{H}_x+2\overline{K}_2\sin\theta_{\mathrm{c}}}\\&+\frac{2\chi_\perp K_1}{m^2}\Bigg)^{1/2}\int\mathrm{d}\overline{\tau}\mathrm{d}^3\overline{\mathbf{r}}\Bigg[\frac{1}{2}\left(\frac{\partial\overline{\delta}}{\partial\overline{\tau}}\right)^2\\&+\frac{1}{2}\left(\overline{\nabla\delta}\right)^2+\frac{1}{4}\left(\sqrt{6\overline{\delta}}^2-\overline{\delta}^3\right)\Bigg].\end{aligned}\tag{18}$$

For the quantum reversal of the Néel vector in a small particle of volume $V\ll r_0^3$, the Néel vector is uniform within the particle and $\overline{\delta}$ does not depend on the space $\overline{\mathbf{r}}$. In this case equation (18) reduces to

$$\begin{aligned}\mathcal{S}_{\mathrm{E}}^{\mathrm{eff}}\left[\overline{\delta}(\overline{\mathbf{r}},\overline{\tau})\right]=&\hbar s\epsilon^{5/4}\sqrt{A}V\left(\frac{\sin\theta_{\mathrm{c}}}{\overline{H}_x+2\overline{K}_2\sin\theta_{\mathrm{c}}}+\frac{2\chi_\perp K_1}{m^2}\right)^{1/2}\\&\times\int\mathrm{d}\overline{\tau}\left[\frac{1}{2}\left(\frac{\mathrm{d}\overline{\delta}}{\mathrm{d}\overline{\tau}}\right)^2+\frac{1}{4}\left(\sqrt{6\overline{\delta}}^2-\overline{\delta}^3\right)\right].\end{aligned}\tag{19}$$

The corresponding classical trajectory satisfies the equation of motion

$$\frac{\mathrm{d}^2\overline{\delta}}{\mathrm{d}\overline{\tau}^2}=\frac{1}{2}\sqrt{6\overline{\delta}}-\frac{3}{4}\overline{\delta}^2.\tag{20}$$

Equation (20) has the instanton solution

$$\overline{\delta}\left(\overline{\tau}\right)=\frac{\sqrt{6}}{\cosh^2\left(3^{1/4}\times2^{-5/4}\overline{\tau}\right)},\tag{21}$$

corresponding to the variation of δ from $\delta=0$ at $\tau=-\infty$, to $\delta=\sqrt{6\epsilon}$ at $\tau=0$, and then back to $\delta=0$ at $\tau=\infty$. The associated classical action is found to be

$$\begin{aligned}\mathcal{S}_{\mathrm{cl}}=&\frac{2^{17/4}\times3^{1/4}}{5}\hbar s\epsilon^{5/4}\frac{\left|\cot\theta_H\right|^{1/6}}{\sqrt{1+\left|\cot\theta_H\right|^{2/3}}}\\&\times\left(\frac{1+\left|\cot\theta_H\right|^{2/3}}{1-\epsilon+2\overline{K}_2\left(1+\left|\cot\theta_H\right|^{2/3}\right)}+\frac{2\chi_\perp K_1}{m^2}\right)^{1/2}.\end{aligned}\tag{22}$$

In the WKB approximation, the tunneling rate Γ of a particle escaping from a metastable state has the relation $\Gamma\exp\left(-B/\hbar\right)$. The WKB exponent B is approximately given by U/ω_{b}, where U is the height of barrier, and ω_{b} is the frequency of small oscillations around the minimum of the inverted potential and characterizes the width of the barrier hindering the decay process. For magnetic quantum tunneling, $\omega_{\mathrm{b}}^2\left(\equiv-\overline{E}_1''\left(\delta_{\mathrm{m}}\right)/M\right)$ is inversely proportional to the effective mass of the magnets, where the mass is induced by the transverse component of magnetic field, and δ_{m} corresponds to the position of the minimum of the inverted potential. For general case, the WKB exponent B should be proportional to the power of the parameter $\epsilon=1-H/H_{\mathrm{c}}$ since the height and the width of barrier are proportional to the power of ϵ. Simple analysis of equation (8) shows that the value of ϵ should be small in order to obtain a large tunneling rate. For this case, we obtain the height of barrier as $\overline{E}_1\left(=U/2K_1V\right)=\sin\left(2\theta_{\mathrm{c}}\right)\left(6\epsilon\right)^{3/2}/27$ at $\delta_{\mathrm{m}}=2\sqrt{6\epsilon}/3$ and the oscillation frequency around the minimum of the inverted potential $-\overline{E}_1\left(\delta\right)$ as $\omega_{\mathrm{b}}=2^{-1/4}\times3^{1/4}\epsilon^{1/4}\omega_0\sqrt{\sin\left(2\theta_{\mathrm{c}}\right)}$, where ω_0 is shown in equation (14b). Then we approximately obtain

the WKB exponent B as

$$B \sim \frac{U}{\omega_{\rm b}} = \frac{2^{9/4}}{3^{7/4}}\hbar s\epsilon^{5/4}\frac{|\cot\theta_H|^{1/6}}{\sqrt{1+|\cot\theta_H|^{2/3}}} \times \left(\frac{1+|\cot\theta_H|^{2/3}}{1-\epsilon+2\overline{K}_2\left(1+|\cot\theta_H|^{2/3}\right)}+\frac{2\chi_\perp K_1}{m^2}\right)^{1/2}, \tag{23}$$

which agrees up to the numerical factor with the result in equation (22) obtained by using the explicit instanton solution.

For a large non-compensation $\left(m \gg \sqrt{\chi_\perp K_1}\right)$, equation (23) reduces to

$$\mathcal{S}_{\rm cl}^{\rm FM} = \frac{2^{17/4}\times 3^{1/4}}{5}\hbar s\epsilon^{5/4}V\frac{|\cot\theta_H|^{1/6}}{\sqrt{1-\epsilon+2\overline{K}_2\left(1+|\cot\theta_H|^{2/3}\right)}}, \tag{24}$$

which agrees well with the result of quantum tunneling of magnetization in single-domain ferromagnetic particles with biaxial symmetry in an arbitrarily directed field [19]. For a small non-compensation $\left(m \ll \sqrt{\chi_\perp K_1}\right)$, equation (23) reduces to the result for single-domain antiferromagnetic particles,

$$\mathcal{S}_{\rm cl}^{\rm AFM} = \frac{2^{17/4}\times 3^{1/4}}{5}\frac{\sqrt{\chi_\perp K_1}}{\gamma}V\epsilon^{5/4}\frac{|\cot\theta_H|^{1/6}}{\sqrt{1+|\cot\theta_H|^{2/3}}}, \tag{25}$$

which is in good agreement with the result in references [20,21].

Now we turn to the nonuniform problem. In case of a thin film of thickness h less than the size $r_0/\epsilon^{1/4}$ of the critical nucleus and its plane is perpendicular to the initial easy axis, we obtain the effective action after performing the integration over the $\overline{\mathbf{z}}$ variable in equation (19),

$$\mathcal{S}_{\rm E}^{\rm eff}\left[\overline{\delta}\left(\overline{\mathbf{r}},\overline{\tau}\right)\right] = \hbar s\epsilon^{3/4}r_0^2 h \times\sqrt{\frac{1}{A}}\left(\frac{\sin\theta_{\rm c}}{\overline{H}_x+2\overline{K}_2\sin\theta_{\rm c}}+\frac{2\chi_\perp K_1}{m^2}\right)^{1/2} \times\int {\rm d}\overline{\tau}{\rm d}^2\overline{\mathbf{r}}\left[\frac{1}{2}\left(\frac{\partial\overline{\delta}}{\partial\overline{\tau}}\right)^2 + \frac{1}{2}\left(\overline{\nabla\delta}\right)^2+\frac{1}{4}\left(\sqrt{6}\overline{\delta}^2-\overline{\delta}^3\right)\right]. \tag{26}$$

At zero temperature the classical solution of the effective action (26) has $O\left(3\right)$ symmetry in two spatial plus one imaginary time dimensions. Therefore, the solution $\overline{\delta}$ is a function of u, where $u=\left(\overline{\rho}^2+\overline{\tau}^2\right)^{1/2}$, and $\overline{\rho}=\left(\overline{x}^2+\overline{y}^2\right)^{1/2}$ is the normalized distance from the $\mathbf{z}$-axis.

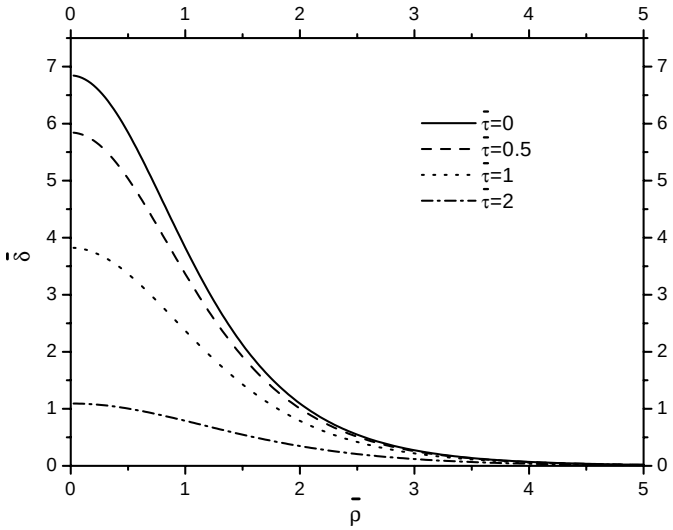

Fig. 1. The instanton, corresponding to subbarrier bubble formation in a thin film by quantum tunneling in a magnetic field with $\pi/2<\theta_H<\pi$, for $\overline{\tau}=0$, $\overline{\tau}=\pm 0.5$, $\overline{\tau}=\pm 1$, and $\overline{\tau}=\pm 2$.

Now the effective action (26) becomes

$$\mathcal{S}_{\rm E}^{\rm eff}\left[\overline{\delta}\left(\overline{\mathbf{r}},\overline{\tau}\right)\right] = 4\pi\hbar s\epsilon^{3/4}r_0^2 h \times\sqrt{\frac{1}{A}}\left(\frac{\sin\theta_{\rm c}}{\overline{H}_x+2\overline{K}_2\sin\theta_{\rm c}}+\frac{2\chi_\perp K_1}{m^2}\right)^{1/2} \times\int {\rm d}u u^2\left[\frac{1}{2}\left(\frac{{\rm d}\overline{\delta}}{{\rm d}u}\right)^2+\frac{1}{4}\left(\sqrt{6}\overline{\delta}^2-\overline{\delta}^3\right)\right]. \tag{27}$$

The corresponding classical trajectory satisfies the equation of motion

$$\frac{{\rm d}^2\overline{\delta}}{{\rm d}u^2}+\frac{2}{u}\frac{{\rm d}\overline{\delta}}{{\rm d}u}=\frac{\sqrt{6}}{2}\overline{\delta}-\frac{3}{4}\overline{\delta}^2. \tag{28}$$

By applying the similar method [5,7], the instanton solution of equation (28) can be found numerically and is illustrated in Figure 1. The maximal rotation of the Néel vector is $\overline{\delta}_{\max}\approx 6.8499$ at $\overline{\tau}=0$ and $\overline{\rho}=0$. Numerical integration in equation (27), using this solution, gives the rate of quantum nucleation for a thin antiferromagnetic film as

$$\Gamma_Q\exp\left(-\mathcal{S}_{\rm E}/\hbar\right)=\exp\left\{-74.39 s\epsilon^{3/4}r_0^2 h \times\frac{\sqrt{1+|\cot\theta_H|^{2/3}}}{|\cot\theta_H|^{1/6}} \times\left(\frac{1+|\cot\theta_H|^{2/3}}{1-\epsilon+2\overline{K}_2\left(1+|\cot\theta_H|^{2/3}\right)}+\frac{2\chi_\perp K_1}{m^2}\right)^{1/2}\right\}. \tag{29}$$

For a large non-compensation, equation (29) reduces to the result for quantum nucleation in a thin ferromagnetic film

$$\Gamma_Q \exp\left(-\mathcal{S}_{\rm E}^{\rm FM}/\hbar\right) = \exp\left\{ -74.39 s\epsilon^{3/4} r_0^2 h \times \frac{1+\left|\cot\theta_H\right|^{2/3}}{\left|\cot\theta_H\right|^{1/6}\sqrt{1-\epsilon+2\overline{K}_2\left(1+\left|\cot\theta_H\right|^{2/3}\right)}}\right\}. \quad (30)$$

For a small non-compensation, equation (29) reduces to the result for quantum nucleation in a thin antiferromagnetic film

$$\Gamma_Q \exp\left(-\mathcal{S}_{\rm E}^{\rm AFM}/\hbar\right) = \exp\left\{ -105.2\frac{\sqrt{\chi_\perp K_1}}{\gamma} \times \epsilon^{3/4} r_0^2 h \frac{\sqrt{1+\left|\cot\theta_H\right|^{2/3}}}{\left|\cot\theta_H\right|^{1/6}}\right\}. \quad (31)$$

At high temperature, the nucleation of the Néel vector is due to thermal activation, and the rate of nucleation follows $\Gamma_T \exp\left(-W_{\rm min}/k_{\rm B}T\right)$, where $W_{\rm min}$ is the minimal work necessary to produce a nucleus capable of growing. In this case the instanton solution becomes independent of the imaginary-time variable $\overline{\tau}$. In order to obtain $W_{\rm min}$, we consider the effective potential of the system

$$U_{\rm eff} = \int {\rm d}^3\mathbf{r}\left[\frac{\alpha}{2}\left((\nabla\theta)^2 + \sin^2\theta\,(\nabla\phi)^2\right) + E\left(\theta,\phi\right)\right]. \quad (32)$$

For a cylindrical bubble equation (32) becomes

$$U_{\rm eff} = 4\pi K_1 \epsilon r_0^2 \int_0^\infty {\rm d}\overline{\rho\rho}\left[\frac{1}{2}\left(\frac{{\rm d}\overline{\delta}}{{\rm d}\overline{\rho}}\right)^2 + \frac{1}{4}\left(\sqrt{6}\overline{\delta}^2 - \overline{\delta}^3\right)\right]. \quad (33)$$

From the saddle point of the functional the shape of the critical nucleus satisfies

$$\frac{{\rm d}^2\overline{\delta}}{{\rm d}\overline{\rho}^2} + \frac{1}{\overline{\rho}}\frac{{\rm d}\overline{\delta}}{{\rm d}\overline{\rho}} = \frac{\sqrt{6}}{2}\overline{\delta} - \frac{3}{4}\overline{\delta}^2. \quad (34)$$

The solution can be found by numerical method similar to the one in references [5,7]. Figure 2 shows the shape of the critical bubble in thermal nucleation, and the maximal size is 3.906 at $\overline{\rho} = 0$. Using this result, the minimal work corresponding the thermal nucleation is

$$W_{\rm min} = 41.3376 K_1 \epsilon r_0^2 h. \quad (35)$$

Comparing this with equation (29), we obtain the approximate formula for the temperature characterizing the crossover from thermal to quantum nucleation as

$$k_{\rm B}T_{\rm c} \approx 0.55\frac{K_1\epsilon^{1/4}}{s}\frac{\left|\cot\theta_H\right|^{1/6}}{\sqrt{1+\left|\cot\theta_H\right|^{2/3}}} \times \left(\frac{1+\left|\cot\theta_H\right|^{2/3}}{1-\epsilon+2\overline{K}_2\left(1+\left|\cot\theta_H\right|^{2/3}\right)} + \frac{2\chi_\perp K_1}{m^2}\right)^{-1/2}. \quad (36)$$

For the FM case, *i.e.*, the case of large non-compensation, the crossover temperature is

$$k_{\rm B}T_{\rm c}^{\rm FM} \approx 0.55\frac{K_1\epsilon^{1/4}}{s}\frac{\left|\cot\theta_H\right|^{1/6}}{\sqrt{1-\epsilon+2\overline{K}_2\left(1+\left|\cot\theta_H\right|^{2/3}\right)}}. \quad (37)$$

While for the AFM case, *i.e.*, the case of small non-compensation,

$$k_{\rm B}T_{\rm c}^{\rm AFM} \approx 0.39\hbar\gamma\sqrt{\frac{K_1}{\chi_\perp}}\epsilon^{1/4}\frac{\left|\cot\theta_H\right|^{1/6}}{\sqrt{1+\left|\cot\theta_H\right|^{2/3}}}. \quad (38)$$

To observe the quantum nucleation one needs a large crossover temperature and not too small a nucleation rate. Note that $\chi_\perp = m_1^2/J_{\rm ex}$ and $m_1 = \hbar\gamma S$ where $J_{\rm ex}$ is the exchange interaction between two sublattices and

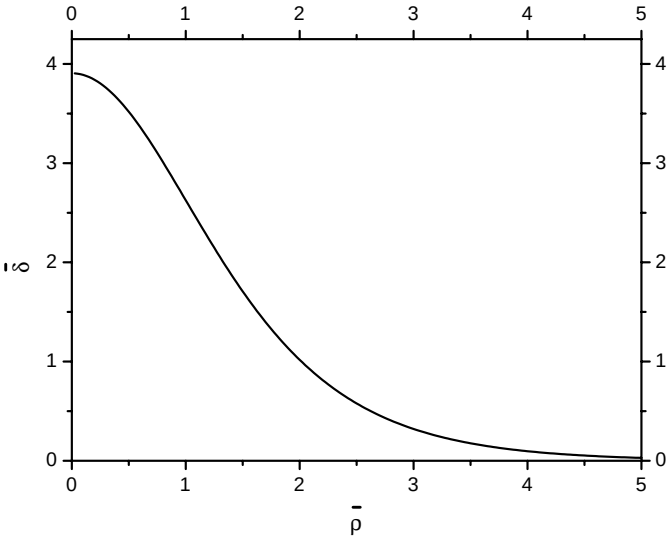

Fig. 2. The shape of the critical bubble in a thermal nucleation of magnetization in a magnetic field with $\pi/2 < \theta_H < \pi$.

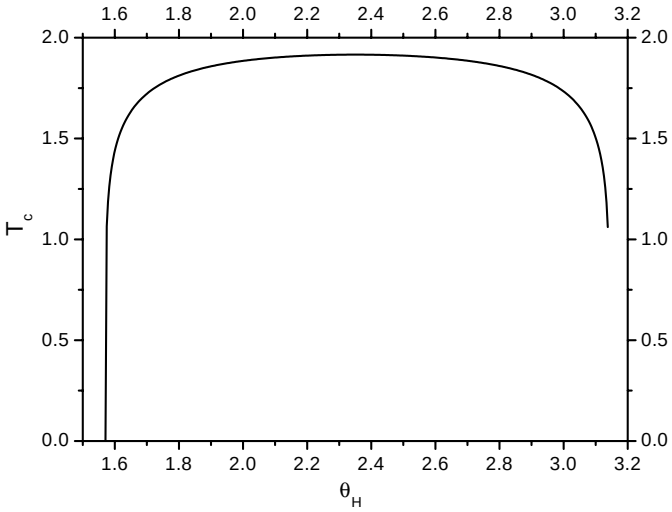

Fig. 3. The θ_H dependence of the crossover temperature T_c for $\pi/2 < \theta_H < \pi$. Here, $K_1 = 10^7$ erg/cm^3, $J_{ex} = 10^{10}$ erg/cm^3, $\overline{K}_2 = 1$, $m = 10$ emu/cm^3, $S/s = 100$, and $\epsilon = 0.01$.

S is the sublattice spin, equation (36) can be written as

$$k_{\rm B}T_{\rm c} \approx 0.55\frac{K_1\epsilon^{1/4}\hbar\gamma}{m}\frac{\left|\cot\theta_H\right|^{1/6}}{\sqrt{1+\left|\cot\theta_H\right|^{2/3}}} \times\left(\frac{1+\left|\cot\theta_H\right|^{2/3}}{1-\epsilon+2\overline{K}_2\left(1+\left|\cot\theta_H\right|^{2/3}\right)}+2\left(\frac{S}{s}\right)^2\left(\frac{K_1}{J_{\rm ex}}\right)\right)^{-1/2}.$$

In Figure 3, we plot the θ_H dependence of the crossover temperature T_c for typical values of parameters for nanometer-scale antiferromagnets: $K_1 = 10^7$ erg/cm^3, $J_{ex} = 10^{10}$ erg/cm^3, $\overline{K}_2 = 1$, $m = 10$ emu/cm^3, $S/s = 100$, $\epsilon = 0.01$ in a wide range of angles $\pi/2 < \theta_H < \pi$. Figure 3 shows that the maximal value of T_c is about 1.916 K at $\theta_H = 2.350$, which is one or two orders of magnitude higher than that for ferromagnets with a similar size [5,7]. Note that, even for ϵ as small as 10^{-3}, the angle corresponding to an appreciable change of the orientation of the Néel vector by quantum tunneling is $\delta_2 = \sqrt{6\epsilon}$ rad$> 4°$. The maximal value of T_c as well as Γ_Q is expected to be observed in experiment.

Now we study the situation that the magnetic field is applied opposite to the initial easy axis, *i.e.*, $\theta_H = \pi$. In this case, $\theta_0 = \theta_c = 0$, $\overline{H}_x = 0$, and $\eta = 0$ from equations (10a, 10b). By using the dimensional variables $\mathbf{r}' = \epsilon^{1/2}\mathbf{r}/r_0$, $\tau' = \epsilon^{1/2}\omega_0\tau$, $\overline{\delta} = \delta/\sqrt{\epsilon}$, where $r_0 = \sqrt{\alpha/2K_1}$, and

$$\omega_0 = \frac{2\gamma K_1}{m}\left(\frac{1}{2\overline{K}_2}+\frac{2\chi_\perp K_1}{m^2}\right)^{-1/2},$$

we obtain the Euclidean action as

$$\mathcal{S}_{\rm E}\left[\overline{\delta}\left(\mathbf{r}',\tau'\right),\phi\left(\mathbf{r}',\tau'\right)\right] = \frac{r_0^3}{\epsilon^2\omega_0}\int {\rm d}\tau'{\rm d}^3\mathbf{r}' \times\left\{\frac{\chi_\perp}{2\gamma^2}\epsilon^2\omega_0^2\left[\left(\frac{\partial\overline{\delta}}{\partial\tau'}\right)^2+\overline{\delta}^2\left(\frac{\partial\phi}{\partial\tau'}\right)^2\right] -{\rm i}\frac{m}{\gamma}\epsilon^{3/2}\omega_0\phi\overline{\delta}\left(\frac{\partial\overline{\delta}}{\partial\tau'}\right)+2K_1\left[\overline{K}_2'\epsilon\overline{\delta}^2\phi^2 +\frac{1}{2}\epsilon^2\left(\nabla'\overline{\delta}\right)^2+\frac{1}{2}\epsilon^2\overline{\delta}^2\left(\nabla'\phi\right)^2+\frac{1}{2}\epsilon^2\left(\overline{\delta}^2-\frac{\overline{\delta}^4}{4}\right)\right]\right\}. \quad (39)$$

The Gaussian integration over ϕ reduces equation (39) to the following effective action

$$\mathcal{S}_{\rm E}^{\rm eff}\left[\overline{\delta}\left(\mathbf{r}',\tau'\right)\right] = \frac{2K_1r_0^3}{\omega_0}\int {\rm d}\tau'{\rm d}^3\mathbf{r}' \times\left[\frac{1}{2}\left(\frac{\partial\overline{\delta}}{\partial\tau'}\right)^2+\frac{1}{2}\left(\nabla'\overline{\delta}\right)^2+\frac{1}{2}\left(\overline{\delta}^2-\frac{\overline{\delta}^4}{4}\right)\right]. \quad (40)$$

In the case of quantum nucleation of the Néel vector in a small particle of volume $V \ll r_0^3$, the Néel vector is uniform within the particle and equation (40) reduces to

$$\mathcal{S}_{\rm E}^{\rm eff}\left[\overline{\delta}\left(\tau'\right)\right] = \frac{2K_1}{\omega_0}\epsilon^{3/2}V\int {\rm d}\tau'\left[\frac{1}{2}\left(\frac{\partial\overline{\delta}}{\partial\tau'}\right)^2+\frac{1}{2}\left(\overline{\delta}^2-\frac{\overline{\delta}^4}{4}\right)\right]. \quad (41)$$

The classical trajectory satisfies the equation of motion

$$\frac{{\rm d}^2\overline{\delta}}{{\rm d}\tau'^2} = \overline{\delta}-\frac{1}{2}\overline{\delta}^3, \quad (42)$$

which has the instanton solution

$$\overline{\delta}\left(\tau'\right) = \frac{2}{\cosh\tau'}, \quad (43)$$

corresponding to the variation of δ from $\delta = 0$ at $\tau = -\infty$, to $\delta = 2\sqrt{\epsilon}$ at $\tau = 0$, and then back to $\delta = 0$ at $\tau = \infty$. Substituting this solution into equation (41) we obtain that

$$\mathcal{S}_{\rm cl} = \frac{8}{3}\hbar s\epsilon^{3/2}V\left(\frac{1}{2\overline{K}_2}+\frac{2\chi_\perp K_1}{m^2}\right)^{1/2}. \quad (44)$$

In the case of quantum nucleation in a thin film of thickness h less than the size $r_0/\sqrt{\epsilon}$ of the critical nucleus with its plane perpendicular to the initial easy axis, the Euclidean action (39) becomes

$$\mathcal{S}_{\rm E}^{\rm eff}\left[\overline{\delta}\left(\mathbf{r}',\tau'\right)\right] = 4\pi\hbar\epsilon^{1/2}r_0^2h\left(\frac{1}{2\overline{K}_2}+\frac{2\chi_\perp K_1}{m^2}\right)^{1/2} \times\int {\rm d}uu^2\left[\frac{1}{2}\left(\frac{{\rm d}\overline{\delta}}{{\rm d}u}\right)^2+\frac{1}{2}\left(\overline{\delta}^2-\frac{\overline{\delta}^4}{4}\right)\right], \quad (45)$$

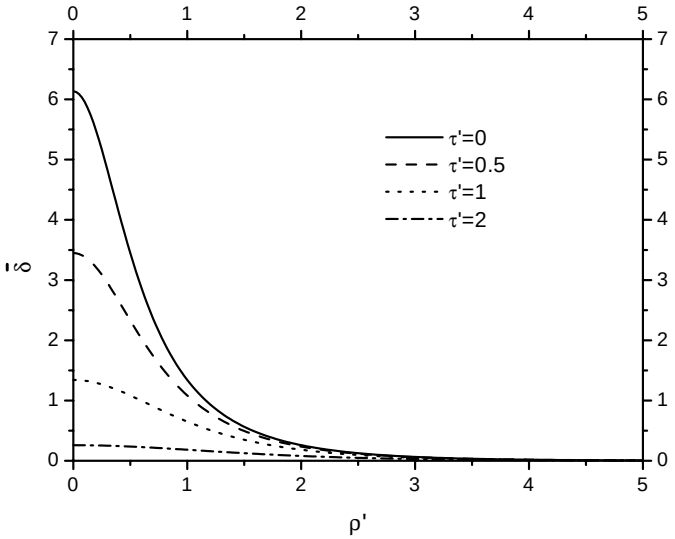

Fig. 4. The instanton, corresponding to subbarrier bubble formation in a thin film by quantum tunneling in a magnetic field with $\theta_H = \pi$, for $\tau' = 0$, $\tau' = \pm 0.5$, $\tau' = \pm 1$, and $\tau' = \pm 2$.

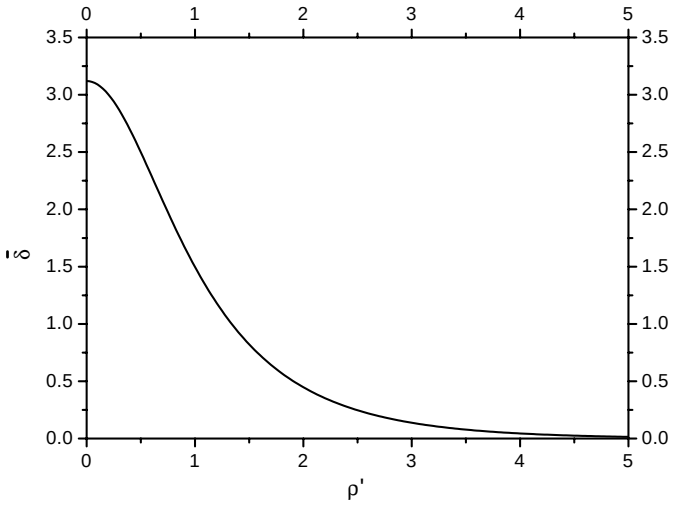

Fig. 5. The shape of the critical bubble in a thermal nucleation of magnetization in a magnetic field with $\theta_H = \pi$.

where $u^2 = \rho'^2 + \tau'^2$, and $\rho'^2 = x'^2 + y'^2$. The corresponding classical equation of motion satisfies

$$\frac{\mathrm{d}^2\overline{\delta}}{\mathrm{d}u^2} + \frac{2}{u}\frac{\mathrm{d}\overline{\delta}}{\mathrm{d}u} = \overline{\delta} - \frac{1}{2}\overline{\delta}^3. \tag{46}$$

The instanton solution of equation (46) can be found numerically and is illustrated in Figure 4. Numerical integration in equation (45), using this solution, gives the WKB exponent for the subbarrier bubble nucleation in an antiferromagnetic film as

$$\Gamma_Q \exp\left(-\mathcal{S}_\mathrm{E}/\hbar\right) = \exp\left\{-37.797 s\epsilon^{1/2} r_0^2 h \left(\frac{1}{2\overline{K}_2} + \frac{2\chi_\perp K_1}{m^2}\right)^{1/2}\right\}. \tag{47}$$

For a cylindrical bubble, the effective potential of the thermal nucleation is found to be

$$U_\mathrm{eff} = 4\pi K_1 \epsilon r_0^2 h \int_0^\infty \mathrm{d}\rho' \rho' \left[\frac{1}{2}\left(\frac{\mathrm{d}\overline{\delta}}{\mathrm{d}\rho'}\right)^2 + \frac{1}{2}\left(\overline{\delta}^2 - \frac{\overline{\delta}^4}{4}\right)\right], \tag{48}$$

wherein the shape of the critical nucleus corresponds to a saddle point of this functional:

$$\frac{\mathrm{d}^2\overline{\delta}}{\mathrm{d}\rho'^2} + \frac{1}{\rho'}\frac{\mathrm{d}\overline{\delta}}{\mathrm{d}\rho'} = \overline{\delta} - \frac{1}{2}\overline{\delta}^3. \tag{49}$$

Equation (49) can be solved by the numerical approach, and the solution is showed in Figure 5. Numerical integration of this solution in equation (48) gives $\Gamma_T \exp\left(-W_\mathrm{min}/k_\mathrm{B}T\right)$ with $W_\mathrm{min} = 23.402 K_1 \epsilon r_0^2 h$. Then the crossover temperature is found to be

$$k_\mathrm{B} T_\mathrm{c} \approx 0.619 \frac{K_1 \epsilon^{1/4}}{s}\left(\frac{1}{2\overline{K}_2} + \frac{2\chi_\perp K_1}{m^2}\right)^{-1/2}. \tag{50}$$

In conclusion, we have investigated the quantum nucleation of the Néel vector in nanometer-scale antiferromagnets with biaxial symmetry in the presence of an external magnetic field at arbitrary angle. By applying the instanton method in the spin-coherent-state path-integral representation, we obtain the analytical formulas for quantum reversal of the Néel vector in small magnets and the numerical formulas for quantum nucleation in thin antiferromagnetic film in a wide range of angles $\pi/2 < \theta_H < \pi$, and $\theta_H = \pi$ respectively. The temperature characterizing the crossover from the quantum to thermal nucleation is clearly shown for each case. Our results show that the rate of quantum nucleation and the crossover temperature depend on the orientation of the external magnetic field distinctly. When $\theta_H = \pi$, the magnetic field is applied antiparallel to the anisotropy axis. It is found that even a very small misalignment of the field with the above orientation can completely change the results of tunneling rates. Another interesting conclusion concerns the field strength dependence of the WKB exponent or the classical action in the rate of quantum nucleation. We have found that in a wide range of angles, the $\epsilon\left(= 1 - \overline{H}/\overline{H}_\mathrm{c}\right)$ dependence of the WKB exponent or the classical action S_cl is given by $\epsilon^{5/4}$, not $\epsilon^{3/2}$ for $\theta_H = \pi$. Therefore, both the orientation and the strength of the external magnetic field are the controllable parameters for the experimental test of quantum nucleation of the Néel vector in nanometer-scale antiferromagnets. If the experiment is to be performed, there are three control parameters for comparison with theory: the angle of the external magnetic field θ_H, the strength of the field in terms of ϵ, and the temperature T.

Recently, Wernsdorfer and co-workers have performed the switching field measurements on individual ferrimagnetic and insulating BaFeCoTiO nanoparticles containing about 10^5–10^6 spins at very low temperatures (0.1–6 K) [22]. They found that above 0.4 K, the magnetization reversal of these particles is unambiguously

described by the Néel-Brown theory of thermal activated rotation of the particle's moment over a well defined anisotropy energy barrier. Below 0.4 K, strong deviations from this model are evidenced which are quantitatively in agreement with the predictions of the MQT theory without dissipation [19,23]. It is noted that the observation of quantum nucleation of ferromagnetic or antiferromagnetic bubbles would be extremely interesting as the next example, after single-domain nanoparticles, of macroscopic quantum tunneling. The experimental procedures on single-domain ferromagnetic nanoparticles of Barium ferrite with uniaxial symmetry [22] may be applied to the antiferromagnetic systems. Note that the inverse of the WKB exponent B^{-1} is the magnetic viscosity S at the quantum-tunneling-dominated regime $T \ll T_c$ studied by magnetic relaxation measurements [2]. Therefore, the quantum nucleation of the antiferromagnetic bubbles should be checked at any θ_H by magnetic relaxation measurements. Over the past years a lot of experimental and theoretical works were performed on the spin tunneling in molecular Mn_{12} -Ac [24] and Fe_8 [25] clusters having a collective spin state $S = 10$ (in this paper $S = 10^6$). Recent progresses in the field of molecular magnets include the measurements of the spin-lattice relaxation rate [30], the specific heat and the Ac-susceptibility on Mn_{12}-Ac [31], the studies of energy sublevels of the ground state by inelastic neutron scattering (INS) [32] and the zero-field magnetic relaxation of Mn_{12}-Ac [33], and the model calculation of the magnetization relaxation based on phonon-assisted tunneling on Mn_{12}-Ac [34]; the INS experiment on Fe_8 [35], the measurement of effects of nuclear spins on the magnetic relaxation of Fe_8 [36], and the nonadiabatic Landau-Zener tunneling in Fe_8 [37,38]. Further experiments should focus on the level quantization of collective spin states of $S = 10^2$–10^4.

The ferromagnet or antiferromagnet is typically an insulating particle with as many as 10^3–10^6 magnetic moments. For the dynamical process, it is important to include the effect of the environment on quantum tunneling caused by phonons [26,27], nucleation spins [28], and Stoner excitations and eddy currents in metallic magnets [29]. However, many studies showed that even though these couplings might be crucial in macroscopic quantum coherence, they are not strong enough to make the quantum tunneling unobservable [2,26–29]. The theoretical calculations performed in this paper can be extended to the antiferromagnetic systems with more general symmetries, such as trigonal, tetragonal and hexagonal symmetries. We hope that the theoretical results presented in this paper may stimulate more experiments whose aim is observing quantum nucleation in nanometer-scale magnets.

R. L. and Y. Z. would like to acknowledge Dr. Su-Peng Kou, Dr. Hui Hu, Dr. Jian-She Liu, Professor Zhan Xu, Professor Mo-Lin Ge, Professor Jiu-Qing Liang and Professor Fu-Cho Pu for stimulating discussions. R. L. and J. L. Z. would like to thank Professor W. Wernsdorfer and Professor R. Sessoli for providing their paper (Ref. [16]). R. L. would like to thank Professor G.-H. Kim for providing his paper (Ref. [21]).

References

1. A.O. Caldeira, A.J. Leggett, Phys. Rev. Lett. **46**, 211 (1981); Ann. Phys. **149**, 374 (1983).
2. For a review, see *Quantum Tunneling of Magnetization*, edited by L. Gunther, B. Barbara (Kluwer, Dordrecht, 1995); and E.M. Chudnovsky, J. Tejada, *Macroscopic Quantum Tunneling of the Magnetic Moment* (Cambridge University Press, 1997).
3. A.P. Malozemoff, J.C. Slonczewski, *Magnetic Domain Walls in Bubble Materials* (Academic, New York, 1979).
4. I.A. Privorotskii, Uspekhi Fiz. Nauk. **108**, 43 (1972) [Sov. Phys. -Usp. **15**, 555 (1973)].
5. E.M. Chudnovsky, L. Gunther, Phys. Rev. B **37**, 9455 (1988).
6. A. Ferrera, E.M. Chudnovsky, Phys. Rev. B **53**, 354 (1996).
7. G.-H. Kim, Phys. Rev. B **55**, 15053 (1998).
8. E.M. Chudnovsky, J. Magn. Magn. Mater. **140-144**, 1821 (1995).
9. I.V. Krive, O.B. Zaslavskii, J. Phys. Cond. Matt. **2**, 9457 (1990).
10. H. Simanjuntak, J. Phys. Cond. Matt. **6**, 2925 (1994).
11. C. Kittle, Rev. Modern Phys. **21**, 552 (1949); E.P. Wohlfarth, Proc. Phys. Soc. (London) A **65**, 1053 (1952); C. Herring, Phys. Rev. **85**, 1003 (1952).
12. D. Loss, D.P. DiVincenzo, G. Grinstein, Phys. Rev. Lett. **69**, 3232 (1992).
13. J.V. Delft, G.L. Henley, Phys. Rev. Lett. **69**, 3236 (1992).
14. A. Garg, Europhys. Lett. **22**, 205 (1993).
15. H.B. Braun, D. Loss, Europhys. Lett. **31**, 555 (1995).
16. W. Wernsdorfer, R. Sessoli, Science **284**, 133 (1999).
17. A. Chiolero, D. Loss, Phys. Rev. B **56**, 738 (1997); Phys. Rev. Lett. **80**, 169 (1998).
18. Rong Lü, Jia-Lin Zhu, Xi Chen, Lee Chang, Euro. Phys. J. B **3**, 35 (1998); Rong Lü, Jia-Lin Zhu, Xiao-Bing Wang, Lee Chang, Phys. Rev. B **58**, 8542 (1998).
19. G.-H. Kim, D.S. Hwang, Phys. Rev. B **55**, 8918 (1997).
20. Rong Lü, Jia-Lin Zhu, Xiao-Bing Wang, Lee Chang, Phys. Rev. B **60**, 4101 (1999).
21. G.-H. Kim, J. Appl. Phys. **86**, 6271 (1999).
22. W. Wernsdorfer, E.B. Orozco, K. Hasselbach, A. Benoit, D. Mailly, O. Kubo, H. Nakano, B. Barbara, Phys. Rev. Lett. **79**, 4014 (1997); W. Wernsdorfer, E.B. Orozco, B. Barbara, A. Benoit, D. Mailly, Physica B **280**, 264 (2000).
23. M.-G. Miguel, E.M. Chudnovsky, Phys. Rev. B **54**, 388 (1996).
24. R. Sessoli, D. Gatteschi, A. Caneschi, M.A. Novak, Nature **365**, 141 (1993); C. Paulsen, J.-G. Park, in *Quantum Tunneling of Magnetization*, edited by L. Gunther, B. Barbara (Kluwer, Dordrecht, 1995); M.A. Novak, R. Sessoli, in *Quantum Tunneling of Magnetization*, edited by L. Gunther, B. Barbara (Kluwer, Dordrecht, 1995); J.M. Hernández, X.X. Zhang, F. Luis, J. Bartolomé, J. Tejada, R. Ziolo, Europhys. Lett. **35**, 301 (1996); L. Thomas, F. Lionti, R. Ballou, D. Gatteschi, R. Sessoli, B. Barbara, Nature (London) **383**, 145 (1996); J.R. Friedman, M.P. Sarachik, J. Tejada, R. Ziolo, Phys. Rev. Lett. **76**, 3820 (1996); J.M. Hernández, X.X. Zhang, F. Luis, J. Tejada, J.R. Friedman, M.P. Sarachik, R. Ziolo, Phys. Rev. B **55**, 5858 (1997); F. Lionti, L. Thomas, R. Ballou, B. Barbara, A. Sulpice, R. Sessoli, D. Gatteschi, J. Appl. Phys. **81**, 4608 (1997); D.A. Garanin, E.M. Chudnovsky, Phys. Rev. B **56**, 11102 (1997).

25. A.-L. Barra, P. Debrunner, D. Gatteschi, C.E. Schulz, R. Sessoli, Europhys. Lett. **35**, 133 (1996); C. Sangregorio, T. Ohm, C. Paulsen, R. Sessoli, D. Gatteschi, Phys. Rev. Lett. **78**, 4645 (1997).
26. E.M. Chudnovsky, L. Gunther, Phys. Rev. Lett. **60**, 661 (1988).
27. A. Garg, G.-H. Kim, Phys. Rev. Lett. **63**, 2512 (1989); Phys. Rev. B **43**, 712 (1991); H. Simanjuntak, J. Low temp. Phys. **90**, 405 (1992).
28. A. Garg, Phys. Rev. Lett. **70**, 1541 (1993).
29. G. Tatara, H. Fukuyama, Phys. Rev. Lett. **72**, 772 (1994).
30. A. Lascialfari, Z.H. Jang, F. Borsa, P. Carretta, D. Gatteschi, Phys. Rev. Lett. **81**, 3773 (1998).
31. A.M. Gomes, M.A. Novak, R. Sessoli, A. Caneschi, D. Gatteschi, Phys. Rev. B **57**, 5021 (1998).
32. I. Mirebeau, M. Hennion, H. Casalta, H. Andres, H.U. Güdel, A.V. Irodova, A. Caneschi, Phys. Rev. Lett. **83**, 628 (1999).
33. L. Thomas, A. Caneschi, B. Barbara, Phys. Rev. Lett. **83**, 2398 (1999).
34. M.N. Leuenberger, D. Loss, Europhys. Lett. **46**, 692 (1999); Phys. Rev. B **61**, 1286 (2000).
35. G. Amoretti, R. Caciuffo, J. Combet, A. Murani, A. Caneschi, Phys. Rev. B **62**, 3022 (2000).
36. W. Wernsdorfer, A. Caneschi, R. Sessoli, D. Gatteschi, A. Cornia, V. Villa, C. Paulsen, Phys. Rev. Lett. **84**, 2965 (2000).
37. W. Wernsdorfer, R. Sessoli, A. Caneschi, D. Gatteschi, A. Cornia, Europhys. Lett. **50**, 552 (2000).
38. M.N. Leuenberger, D. Loss, Phys. Rev. B **61**, 12200 (2000).